Available online at www.sciencedirect.com
ScienceDirect
Acta Biomaterialia 4 (2008) 1288–1296
Acta BIOMATERIALIA
www.elsevier.com/locate/actabiomat

Adhesion between biodegradable polymers and hydroxyapatite: Relevance to synthetic bone-like materials and tissue engineering scaffolds

R.E. Neuendorf [a,b], E. Saiz [b], A.P. Tomsia [b], R.O. Ritchie [a,b,*]

[a] Department of Materials Science and Engineering, University of California, Berkeley, CA 94720, USA
[b] Materials Sciences Division, Lawrence Berkeley National Laboratory, Berkeley, CA 94720, USA

Received 5 March 2008; received in revised form 8 April 2008; accepted 16 April 2008
Available online 28 April 2008

Abstract

Many studies are currently underway on the quest to make synthetic bone-like materials with composites of polymeric materials and hydroxyapatite (HA). In the present work, we use wetting experiments and surface tension measurements to determine the work of adhesion between biodegradable polymers and HA, with specific reference to the role of humid environments. All the polymers are found to exhibit low contact angles ($\leqslant 60°$) on the ceramic with work of adhesion values ranging between 48 J m^{-2} for poly(ε-caprolactone) and 63 J m^{-2} for polylactide; these values are associated with physical bonding across the organic/inorganic interface. The corresponding mechanical fracture strengths, measured using four-point bending tests of HA–polymer–HA bonds, scale directly with the results from the wetting experiments. Short-time aging (up to 30 h) in a humid environment, however, has a dramatic influence on such HA/polymer interfacial strengths; specifically, water diffusion through the organic/inorganic interface and degradation of the polymer results in a marked decrease, by some 80–90%, in the bond strengths. These results cast doubt on the use of biodegradable polymers/ceramic composites for load-bearing synthetic bone-like materials, as desired optimal mechanical properties are unlikely to be met in realistic physiological environments.
Published by Elsevier Ltd. on behalf of Acta Materialia Inc.

Keywords: Synthetic bone-like materials; Biodegradable polymers; Hydroxyapatite; Work of adhesion; Interfacial strength

1. Introduction

The search for strong artificial implants able to perform in load-bearing situations, such as hip or knee replacements, has led to the use of materials that have largely been developed for other, more traditional, engineering applications; such materials include stainless steels, cobalt–chromium alloys, titanium and its alloys, and structural ceramics, such as alumina or zirconia, that are not only stronger than the bone they replace but, more importantly, much stiffer [1,2]. This difference in stiffness is the genesis of many failed implants; living bone is responsive to its environment and implants that are stiffer than bone bear a greater proportion of the load, shielding the surrounding tissue from its normal stress levels. The result of such "stress shielding" is that the surrounding tissue is resorbed and the implant becomes loose over time, often requiring revision surgery [3]. In order to overcome these limitations, over the last years there has been increasing interest in the development of strong organic/inorganic composites that would combine the flexibility, toughness and bioresorbability of a polymer with the stiffness, strength and osteoconductivity of a ceramic. These materials have been investigated for their use in load-bearing situations as bone substitutes or in tissue engineering scaffolds [4–11]. Their advantage is

* Corresponding author. Address: Department of Materials Science and Engineering, University of California, Berkeley, CA 94720, USA. Tel.: +1 510 486 5798.
E-mail address: RORitchie@lbl.gov (R.O. Ritchie).

1742-7061/$ - see front matter Published by Elsevier Ltd. on behalf of Acta Materialia Inc.
doi:10.1016/j.actbio.2008.04.006

that biodegradable polymers would allow for bone growth into degraded sections and further permit load transfer from the implant to the bone, thereby lessening the effect of stress shielding [7–10]. Drug delivery capabilities could also be incorporated by using the biodegradable polymers to slowly release diverse chemicals and growth factors as they degrade [12,13]. Perhaps the most commonly studied composites are hydroxyapatite (HA)-based materials. Synthetic HA [$Ca_{10}(PO_4)_6(OH)_2$] is closely related to the carbonated apatite that constitutes the mineral component of bone (in carbonated apatite the hydroxyl ions are partly displaced by carbonate ions); it is osteoconductive when porous and believed to aid bone formation in vivo [9]. While its bioactive properties make it an ideal material for synthetic bone, its very low fracture toughness and high elastic modulus (Table 1) make necessary for it to be combined with a less stiff ductile material in the form of an organic/inorganic composite. In such composites, HA is frequently combined with polymers based on lactic and glycolic acids or poly(ε-caprolactone) (PCL) [4–11]. These polymers are approved by the Food and Drug Administration (FDA) for use in medical applications owing to their biodegradability, but their low stiffness and, in many cases, poor strength limit their use predominantly to a limited number of non-load-bearing applications.[1]

Several studies have investigated the synthesis and characterization of hybrid HA/polymer materials, and in particular analyzed the effect of the mineral content and the processing route on the mechanical strength and toughness [4–8,10]. However, a detailed analysis leading to an optimization of microstructure is still lacking. Of particular relevance is that the internal interfaces in these microstructures invariably provide the weakest links for the nucleation of cracks that lead to premature failure; consequently the bond strengths of the biomaterial interfaces in such hybrid materials are critical parameters that must be characterized and controlled. Accordingly, in this work, we specifically examine the HA/polymer interface using surface tension and contact angle measurements to estimate the interfacial work of adhesion; in addition, parallel four-point bending tests are used to determine the corresponding mechanical fracture strengths. The experimental conditions (temperature and atmosphere) for the surface tension and contact angle measurements, as well as the preparation of four-point bending specimens, are similar to those commonly used to fabricate HA/polymer composites by hot pressing or injection molding [5–8,10]. Our goal is to assess the strength of "practical" polymer–ceramic bonds and to explore its correlations with fundamental interfacial properties. Emphasis is given to the effect of the environment, principally that of water, on the magnitude of the organic/inorganic bonding.

[1] For applications that are load-bearing, these materials ideally need to display mechanical properties comparable with that of bone, i.e. a stiffness (Young's modulus) of 15–25 GPa, a strength of ~100 MPa and a fracture toughness on the order of 4–8 MPa$\sqrt{m}$.

2. Experimental procedures

We focus in this work on the bonding of HA to several biodegradable polymers, namely poly(L-lactide) (LPLA), poly(D-lactide) (DPLA), poly(DL-lactide) (PDA), 75/25 PDL/polyglycolide (75/25 PDL/PG), 50/50 PDL/polyglycolide (50/50 PDL/PG) and PCL. All have been approved by the FDA for implanting into the human body. Moreover, in combination with HA and other calcium phosphates or bioactive glasses, they are the basis of many studies to develop hybrid organic/inorganic composites and scaffolds with mechanical properties matching those of the host tissue. Selected physical and mechanical properties of the polymers used in this work, together with that of HA, are listed in Table 1.

The surface tension of the polymers, γ, and its dependence with temperature was measured using the pendant drop method. The polymers were melted in a heated syringe whose tip was placed in a heating chamber (Ramé-Hart, USA). A drop was formed and an image was recorded every 10 s using an automated CCD camera. The shape of the pendant drop is dictated by the competition between the surface tension and gravity [14]. The drop profile was analyzed using commercial software (DropImage, Ramé-Hart) in order to calculate the surface energy. Three separate drops of each polymer were measured at each temperature and a minimum of 10 pictures were analyzed for each drop.

Wetting experiments were conducted on dense, polished HA substrates using the sessile drop configuration. To prepare the substrates, a commercial HA powder (Alfa Aesar, USA) was calcined at 1000 °C to remove any excess chemicals that may be present from the synthesis process and to reduce the surface area. The calcined powder was uniaxially pressed at ~100 MPa into cylindrical pellets (10 mm diameter, ~2–3 mm height) and then cold isostatically pressed at ~100 MPa. Then the pellets were sintered in air at 1150 °C for 2 h. The phases present in the sintered substrates were identified by X-ray diffraction (D500, Siemens AG, Munich, Germany); their density was measured using the Archimedes method and their microstructure analyzed by environmental scanning electron microscopy (S-4300SE/N, Hitachi, Japan). The substrates were polished with diamond solution to a 1 μm finish, cleaned with acetone and ethanol, and fired in air at 500 °C for 1 h to further remove any contaminants. The substrates were then placed into a heating chamber with a small piece of polymer on top (~2–4 mm^3) and the assembly was heated to the test temperature. After melting the polymer, in situ images of the sample were taken every 10 s with a CCD camera and analyzed using the DropImage software in order to measure the contact angle. The samples were maintained at the test temperature for times up to 6 h. The assemblies (polymer plus substrate) were weighed before and after the test in order to assess the degree of polymer degradation.

Table 1
Summary of the physical/mechanical properties of the materials used in this study

Materials		Molecular weight (Da)	Density (g cm^{-3})	Melting point (K)	Tensile strength (MPa)	Young's modulus (GPa)	Degradation time (months)
Polymers	LPLA[a]	108,600	1.25–1.3	456.4–466.7	50–60	3–5	>24
	DPLA[a]	107,300	1.24	443.3–452.5	50–60	3–5	>24
	PDL[b]	88,400	1.25	Amorphous	28–41	1.38–2.75	12–16
	75/25 PDL/PG[b]	104,500	1.30	Amorphous	41–55	1.38–2.75	4–5
	50/50 PDL/PG[b]	49,900	1.34	Amorphous	41–55	1.38–2.75	1–2
	PCL[c]	80,000	1.145	333	15–30	0.15–0.3	0.5–1
Ceramic	HA	–	3.2		100–900	35–120	–

The values were obtained from the manufacturers and Refs. [9,11,32–35].
[a] Purasort (Purac).
[b] Absorbable Polymers International.
[c] Aldrich.

The temperature range for the surface tension and contact angle measurements were selected on the basis of the polymer melting temperatures and by physical observation. The melting ranges for Purasorb DPLA and Purasorb LPLA are 443–453 and 456–467 K, respectively; the melting point for PCL is 333 K. As the other polymers are amorphous, no melting temperatures are reported. The choice of temperature became more of an issue with the contact angle measurements as the spreading times are long (of the order of minutes to even hours) and prolonged testing times can lead to polymer degradation. An example of the spreading data is shown in Fig. 1. An empirical exponential decay fitting was used to calculate the equilibrium contact angle (θ_0). Due to the large viscosity of the polymer melts, the contact angles can take more than 1 h to reach an equilibrium value (θ_0). In the present experiments, as no significant weight losses were recorded during these wetting experiments even after 8 h at the test temperature, the polymers can be assumed to have not undergone any significant degradation.

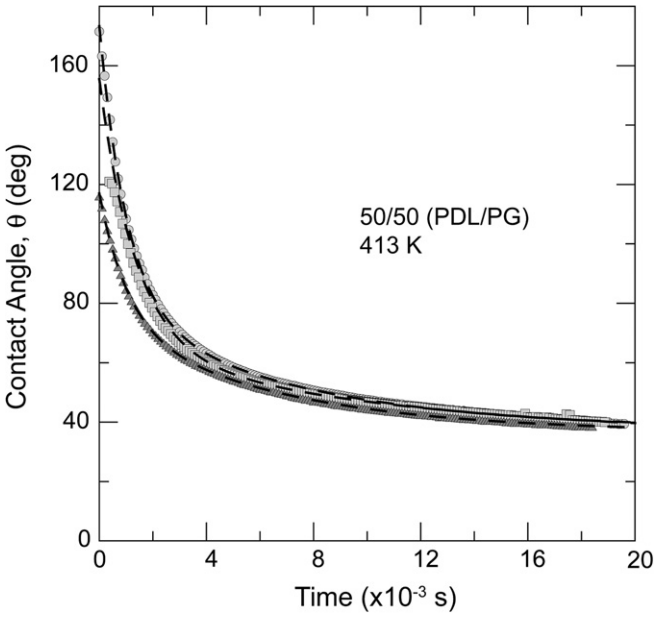

Fig. 1. Evolution of the contact angle of 50/50 (PDL/PG) polymer on HA substrates fired in air at 500 °C after polishing. Each symbol corresponds to a different run. The data are very reproducible. The lines show the empirical exponential decay fittings $\theta = \theta_0 + e^{-t/A} + e^{-t/B}$ used to calculate the equilibrium contact angles as $t \to \infty$, θ_0.

The bonding strength at the polymer/ceramic interface was initially evaluated qualitatively using a crack indentation method developed by Becher et al. [15] whereby cracks are generated by indentation and are propagated towards the interface at different impingement angles to discern whether they penetrate or are arrested at the interface. These cracks were examined in the scanning electron microscope (SEM), the crack path, i.e. the interfacial deflection or penetration into polymer, and the interface debond length, l_{db}, being recorded. With this technique, a critical value of impingement angle was measured below which the crack will deflect along the interface and above which it will propagate through it; the interfacial bonding energy can then be considered to be lower with increasing critical angle. Direct measurements of the interfacial strength, σ_f, were subsequently made quantitatively by loading to failure small rectangular cross-section beams in pure (four-point) bending.

For the indentation crack tests ($N = 20$), cross-sections were cut from the samples used in the wetting experiments to expose the interface between the HA and the polymer. These samples were mounted in resin and polished to a 6 μm finish. Vickers hardness indents were made in the HA approximately 100 μm from the interface using a microhardness tester (Micromet, Buehler, USA). Three to five indents were made on each sample with loads ranging between 100 and 500 g in order to generate corner cracks that would propagate towards the polymer/HA interface and impinge onto it. The sample was rotated at a different angle for each indent such that the incidence angle of the crack would be different. Several indents were discarded due to either lack of well-defined corner cracks or the crack hitting a defect before reaching the interface (~30%). Those cracks that did reach the interface would either

arrest at the interface, travel along it or penetrate into the polymer. Crack trajectories were examined using optical microscopy and a high-resolution environmental SEM to record the incidence angle and the crack path.

In order to prepare samples for the four-point bend tests ($N = 10$), HA substrates were prepared in the same way as the contact angle experiments. The substrates were cut into bars at least 12 mm in length with a cross-section 2–3 mm by 2–3 mm. The bars were then cut in half and the bonding surfaces were polished with SiC to 1200 grit. A drop of polymer was melted on the polished surfaces and the HA bars were bonded in liquid-state at temperatures similar to those used in the wetting tests with no external pressure. Once the samples were made, bend tests were performed immediately (to prevent any contamination or moisture in the environment from affecting the results) using an EnduraTec ELF 3200 voice-coil actuated mechanical testing machine (Bose, Eden Prairie, MN), operating at a crosshead speed of 0.01 mm s^{-1}; the peak load at fracture instability was then used to determine the bond strength, σ_f. Fracture surfaces were subsequently observed by SEM.

The effect of moisture on interfacial adhesion was assessed by pre-soaking the bend samples ($N = 5$) in water vapor (specifically on a pedestal in a sealed container with water) at ambient body temperature (37 °C) for times up to 30 h, and then determining the σ_f four-point bend strength as before. Water was used in these experiments, rather than simulated body fluid or Hanks' balanced saline solution, because we specifically wanted to isolate the effect of the water molecule on the interfacial bonding; accordingly, our experiments involved exposure to a humid environment rather than full immersion in a solution.

3. Results and discussion

3.1. Work of adhesion and spreading

Results showing the measured surface tensions, γ, of the different polymers and copolymers examined in this study are shown in Table 2; values lie between 25 and 40 mJ m^{-2}, which is in the range expected for these materials [16]. The two forms of polylactide (L- and D-) display nearly the same surface tension, which is expected as the two polymers are stereoisomers of each other with no other differences in properties. The racemic form of polylactide (PDL) has a slightly higher value whereas the addition of polyglycolide as a copolymer to PDL lowers the surface tension.

Table 2
Surface tension properties of the different polymers used in this study

Polymer	Temperature, T (K)	Surface tension, γ (mJ m^{-2})	$d\gamma/dT$ (mJ K^{-1} m^{-2})
PDL	453	33.3 ± 0.5	−0.035
75/25 PDL/PG	433	30.6 ± 0.1	−0.036
50/50 PDL/PG	393	32.0 ± 0.8	−0.052
DPLA	478	28.8 ± 0.1	−0.020
LPLA	478	28.9 ± 0.3	−0.050
PCL	393	32.5 ± 0.3	−0.010

The dependence of the polymer surface tension values with temperature can be described in terms of the Guggenheim equation [16], which was originally developed for small-molecule liquids, viz.

$$\gamma = \gamma_0 \left(1 - \frac{T}{T_c}\right)^{11/9} \quad (1)$$

where γ_0 is the surface tension at 0 K and T_c is the critical temperature. Fitting the biopolymer data to Eq. (1) results in T_c values of the order of 1000–2000 K. Correspondingly, for the range of temperatures used in this work the surface tension is approximately linear with temperature T, with the value of $-(d\gamma/dT)$ ranging between 0.01 and 0.055 mJ K^{-1} m^{-2} (Table 2 and Fig. 1), again as expected for polymers, where $-(d\gamma/dT)$ is typically on the order of 0.05 mJ K^{-1} m^{-2} [14,16]. Due to the conformational restrictions of long-chain molecules, the temperature dependence of the surface tension for polymer is usually smaller than for small-molecule liquids (where $-(d\gamma/dT) \sim 0.1$ mJ K^{-1} m^{-2}) [16] (see Fig. 2).

Measurements of the surface tension of the polymers, γ, and the equilibrium contact angles, θ_0, on HA in air are listed in Table 3. The contact angle values on the substrates fired at 500 °C in air are very reproducible (Fig. 1). There was much more variability (up to 30°) on the contact angles measured on HA substrates that were not fired after polishing. As this could be due to the presence of impurities on the HA surface after polishing and cleaning with different organics (which can only be eliminated by firing), the latter values have not been used here. It has been previously observed that the thermal treatments are necessary to clean

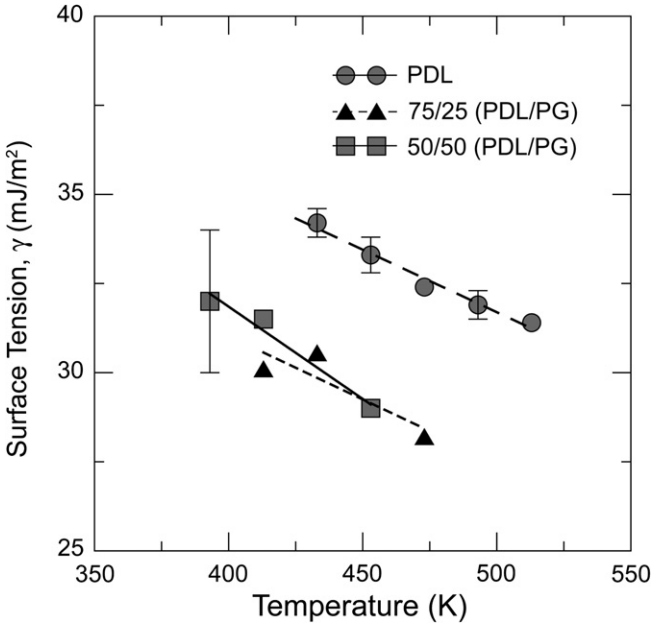

Fig. 2. Measured temperature dependence of the surface tension of the biodegradable polymers.

Table 3
Work of adhesion and contact angles on HA for different polymers

Polymer	Temperature, T (K)	Work of adhesion, W_{ad} (mJ m^{-2})	Contact angle, θ (deg)	Polymer/HA bending strengths, σ_f (MPa)
PDL	453	63 ± 2	28 ± 1	23 ± 2
75/25 (PDL/PG)	433	60 ± 1	18 ± 3	17 ± 1
50/50 (PDL/PG)	393	58 ± 1	37 ± 3	15 ± 4
DPLA	478	56 ± 2	16 ± 5	19 ± 5
LPLA	478	57 ± 1	17 ± 2	20 ± 4
PCL	393	48 ± 3	62 ± 4	9 ± 2

surfaces and improve the wetting of polymers on bioactive glasses [17]. These values were used to calculate the thermodynamic work of adhesion, W_{ad}, using the standard Young–Dupré relationship [14]

$$W_{ad} = \gamma(1 + \cos\theta_0) \quad (2)$$

Computed W_{ad} values, which range between 48 and 63 mJ m^{-2}, are listed in Table 3.

Temperature can be seen to have a minimal effect on the work of adhesion values. An increase in temperature decreases the contact angle, which in turn increases the work of adhesion; however, this is countered by a decrease in surface tension. The trends are similar to those observed with the surface tension. These values of work of adhesion are usually attributed to the formation of a physical bond (e.g. van der Waals and dispersion forces) at the organic/inorganic interface and the absence of interfacial chemical bonding [14,16,18].

3.2. Bonding

Results from the crack indentation method to qualitatively assess the interfacial debonding behavior are shown in Fig. 3. Specifically, for indentation cracks impinging on the polymer/HA interface, the interfacial debond lengths, l_{db}, are plotted as a function of the crack impingement angles, ϑ. From these data, it is apparent that PDL had the lowest critical crack angle (~7°), followed by 75/25 PDL/PG (~12°) then 50/50 PDL/PG (~26°), implying that the addition of polyglycolide as a copolymer to PDL decreases the interfacial debonding energy with HA [19,20].[2] These trends are consistent with the four-point bend measurements described below.

Although the crack indentation method yields qualitative information on the relative strengths of these polymer/HA interfaces, quantitative evaluation of the bonding strengths is best achieved using mechanical testing, e.g. four-point bending tests. Using such test techniques, measured bond strengths were found to range from 9 to 25 MPa; specific values are listed in Table 3. Fracture was found to always occur at the polymer/ceramic interface. An excellent match can be observed between the polymer and ceramic surfaces, indicative of the formation of good interfaces (Fig. 4a). Corresponding applied bending load vs. displacement curves display linear elastic behavior with little evidence of plastic/inelastic deformation prior to catastrophic brittle fracture (Fig. 5a). Measured bond strengths, σ_f (Table 3), are consistent with the formation of a physical bond at the organic/inorganic interface. Physical bonding is common at polymer/ceramic interfaces [16] and frequently ceramic grafting is used to enhance adhesion in hybrid composites (e.g. dental composites). The results follow the trends already observed in the measured work of adhesion values (Table 3). Specifically, whereas poly(L-lactide) and poly(D-lactide) have similar bond strengths to HA, the PDL/HA bond is some 20% stronger and almost a factor of three stronger than the PCL/HA bond. The addition of the glycolide polymer clearly decreases the adhesion of PDL to HA.

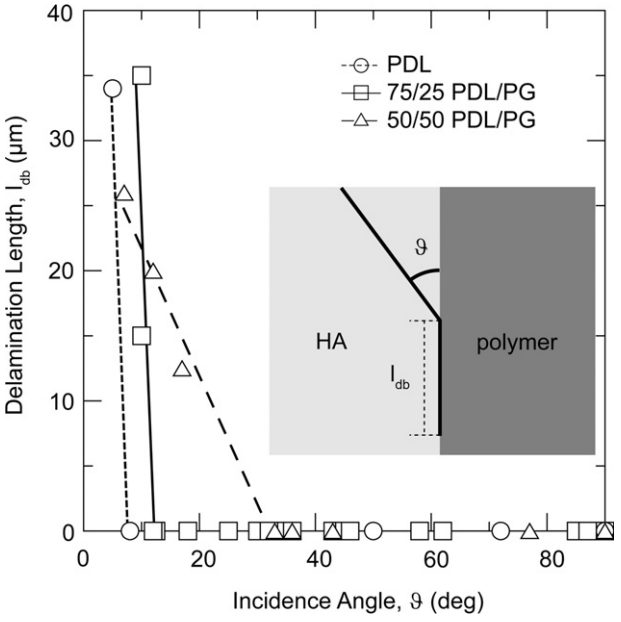

Fig. 3. Crack indentation results showing debond lengths, l_{db}, plotted as a function of the critical incidence angle, v, for cracks impinging on the HA/polymer interfaces.

[2] It is possible with this technique to quantitatively estimate the fracture toughness of the interface, as has been achieved, for example, for the dentin–enamel junction in human teeth [20]. However, this was not feasible in the present instance due to the extreme mismatch of elastic properties across the interface. Specifically, the first Dundurs' parameter, which describes this mismatch and is defined as $\alpha = (E_{HA} - E_P)/(E_{HA} + E_P)$, where E_{HA} and E_P are the respective Young's moduli of HA and the polymer, is of the order of unity ($E_{HA} >> E_P$), making estimates virtually impossible.

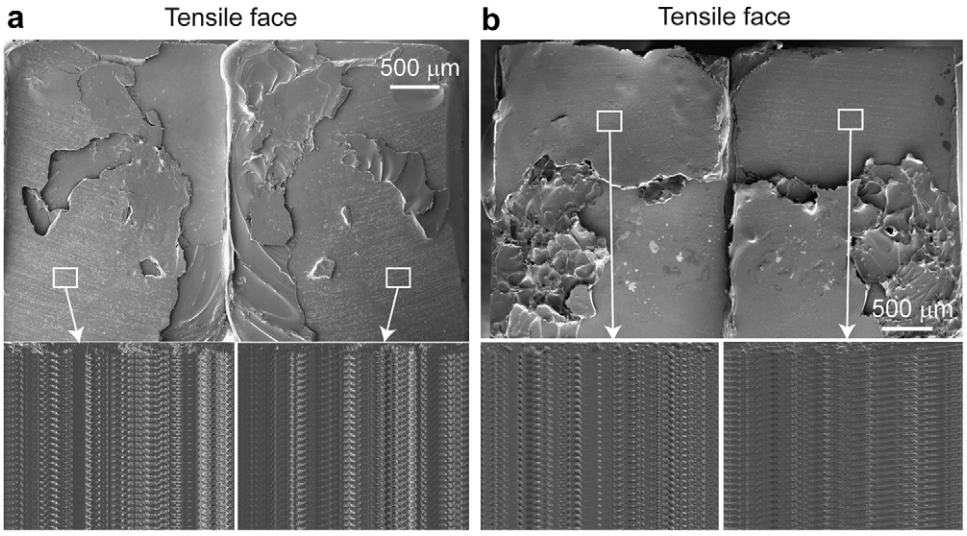

Fig. 4. SEM micrographs of the fracture surfaces after four-point bend testing of (a) 50/50 PDL/PG sample "as-prepared" and (b) the same polymer bond after aging for 30 h in a humid environment at 37 °C. The similar marks found in the polymer and ceramic side of the "as-prepared" joints indicate good bonding. After aging, the surfaces no longer mirror each other. The polymer surface shows clear signs of deformation (indicated by the white arrows).

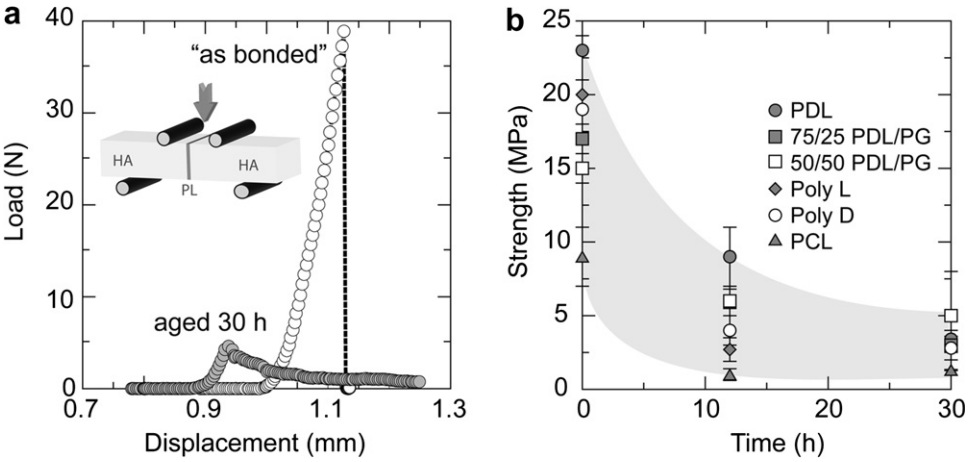

Fig. 5. (a) Load–displacement curves for bending tests on the PL/HA bonds, in the "as-prepared" and after 30 h in a humid environment conditions and (b) observed decrease in the bond strength for the various polymers as a function of aging time in a humid environment.

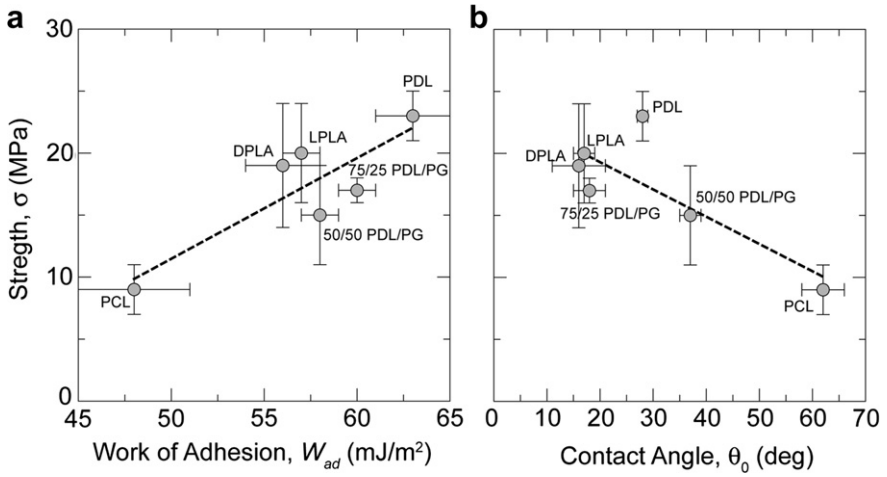

Fig. 6. Relationships between the measured four-point bending interfacial fracture strength and the work of adhesion (a) and contact angle (b) for polymer/ceramic bonds.

Values of the σ_f interfacial bond strengths for the various HA/polymer interfaces are plotted in Fig. 6 as a function of the W_{ad} work of adhesion values and the equilibrium contact angles, θ_0. Relationships between the work of adhesion and the interface strength have been noted previously by several other researchers [21,22]. Indeed, the correlation can be deduced from simple fracture mechanics notions, where the fracture strength, σ_f, is considered to depend upon the fracture energy (strain energy release rate), G_c, as

$$\sigma_f = q\left(\frac{G_c E^*}{c}\right)^{\frac{1}{2}} \tag{3}$$

where E^* is the appropriate modulus [23], c is the flaw size, and the factor q depends upon flaw geometry and includes effects of stress concentrations [24,25] (if σ_f is the nominal strength). There are two contributions to the interfacial fracture energy, one from the adhesion and the other from the plastic dissipation. Although the contribution of plasticity is usually far larger than that of the work of adhesion, it is crack growth that $G_c \propto W_{ad}$ [23,26], such that σ_f will scale with W_{ad}. However, the interfacial bond strength is a function of both chemical and mechanical considerations. A key issue is that the strength is dictated by the worst flaw, which derives from statistically variable processing and machining defects plus low G_c paths, taken relative to local driving forces. Interfacial pores can represent the major strength-limiting flaws, and the formation of a strong bond requires their elimination. The contact angle is a key parameter that dictates the choice of bond processing techniques as it controls interfacial flaw shape and pore removal rate. Lower contact angle values will result in faster removal of interfacial flaws and more benign pore shapes. The effect of W_{ad} or the related θ_0 on the controlling flaw geometry may also account for the empirical correlations between σ_f and W_{ad} [27].

These results suggest that a positive trend exists between σ_f and W_{ad} values for most of the data in Fig. 6a. Thus, this plot seems to affirm that crack-tip chemistry, as described by the work of adhesion, plays a dominant role in controlling bond strength. Alternatively, the inverse correlation between σ_f and θ_0 (Fig. 6b) may reflect the primary influence of interfacial flaw size and shape. In the present case, the measured fracture strengths are of the order of the yield strengths of the polymers, implying that the extent of crack-tip plasticity exceeds the flaw size and small-scale yielding conditions do not apply. It is likely that the interface flaws are blunted and extend by a ductile interfacial fracture mechanism, thereby affirming that the strength-controlling flaws are more potent in dissimilar material bonds with larger contact angles. The comparison between parts (a) and (b) of Fig. 6 may suggest that the dependence with the contact angle is weaker and that, despite the extent of crack-tip plasticity, the strength of the bond scales mostly with the thermodynamic work of adhesion, as has also been qualitatively suggested by the indentation experiments. However, there is still some variability in the measured strengths due, among other things, to the statistical distribution of interfacial flaw sizes (Eq. (3)) that precludes a more quantitative evaluation. Here we have discussed some of the critical factors that control the interfacial strength and showed some preliminary trends that agree with those observed in other systems [21,22,27]. Future assessments could involve an analysis of the interfacial fracture toughness to define quantitatively the effect of the fabrication conditions and their role in determining flaw distribution.

3.3. Environmental effects

Since all the polymers in this study are bioabsorbable, degradation of the polymer in water will occur over time. This will result in the polymer losing strength and stability in the implant. It is well known that organic/inorganic joints can be weakened by exposure to humid environments and that, in some cases (in particular, for hydrophilic phases), migration of water or vapor through the interface can cause spontaneous degradation [16]. It was observed, while working with biopolymers, that moisture could be playing a role in the interfacial bonding to HA; for example, when preparing samples for bend strength tests, cutting and polishing of samples using water as a coolant often resulted in spontaneous detachment at the organic/inorganic interface. In order to quantify these observations, experiments were performed where the samples were aged in a humid environment at 37 °C.

The result of these experiments was that the measured bond strengths were seen to decrease noticeably after 12 h. Although the bending load vs. displacement curves were qualitatively similar to those for the "as-prepared" samples, the HA/polymer interfacial fracture strengths were significantly lower, with the HA/LPLA and HA/DPLA bonds showing the largest drop in fracture strength by almost an order of magnitude to a mere ~3 MPa. PDL had the highest strength value after 12 h in humidity, followed by both 50/50 PDL/PG and 75/25 PDL/PG (Fig. 5b). Fracture was still seen to occur at the polymer/ceramic interface, with good matching between the polymer and ceramic fracture surfaces. However, after 30 h of exposure to humidity, measured bond strengths were seen to have degraded by as much as 80–90%, with marked differences in the load vs. displacement curves. Specifically, stable crack-growth was observed at low applied bending loads, with fractographic evidence of polymer deformation (Fig. 4b), as compared to the "as-prepared" samples, which were far more brittle and fractured catastrophically at peak load (Fig. 5a).

It is clear here that the lack of a strong interfacial chemical bonding at the organic/inorganic interface results in fast degradation of the bond. The hydrophilic nature of the polymer promotes the diffusion of water through the interface [16]; coupled with the polymer biodegradability, this results in a significant degradation of the organic/inorganic bond in the presence of an aqueous environment.

The present results are of particular relevance to the development of synthetic bone-like composites and tissue engineered scaffolds. It is well known that the nature of the internal interfaces, both with respect to their morphology and chemical composition, and their strength relative to the other components of the structure, play a major role in dictating the overall bulk mechanical response of materials, most especially composites. In more brittle materials, the interfaces within a microstructure invariably provide the weakest links for the nucleation of cracks that lead to fracture and premature failures. Results of the present work provide information on the relative strengths of the organic/inorganic interfaces for HA bonded to currently FDA-approved biodegradable polymers for the development of biomaterial composites. Of particular importance are the observations of the major (~80–90%) reductions in bond strength in the prolonged presence of moisture. It has been observed that bulk polymer degradation after immersion in water-based solutions results in a significant decrease in the mechanical properties of biodegradable polymers [28–30]. The results described in this paper indicate that exposure to a humid environment will cause degradation of the bonding at organic/inorganic interfaces that can severely compromise the mechanical response of HA/polymer composites, thereby affecting their stability in vivo before resorption occurs. These results are consistent with previous observations of the mechanical response of such composites after aging [5,6,11,31] and suggest that different strategies must be used to manipulate the microstructure and interfacial bonding in order to ensure stability.

4. Conclusions

Adhesion between calcium phosphates (HA) and biopolymers is controlled by physical interactions. In the present study, HA was bonded to several FDA-approved biodegradable polymers, namely poly(L-lactide), poly(D-lactide), poly(DL-lactide), 75/25 PDL/polyglycolide, 50/50 PDL/polyglycolide and poly(ε-caprolactone); these materials are commonly used for the development of many synthetic bone-like composites and tissue engineered scaffolds. All biopolymers were seen to exhibit low contact angles ($\leqslant 60°$) on the HA ceramic facilitating liquid-state bonding. Corresponding work of adhesion values were found to lie in the range of 48–63 mJ m^{-2}, and to scale roughly with the surface tension of the polymer. Using four-point bend tests, measurements of the mechanical fracture strengths of the HA/polymer bonds were found to be on the order of 9–25 MPa, and to scale with the work of adhesion; mechanical strengths also appear to show an apparent inverse relation to the contact angles. However, on exposure to humid environments, major degradations in the strength of these organic/inorganic interfaces were apparent. In particular, reductions in the bond strength of ~80–90% were observed after aging in water vapor for 30 h. It is believed that such water-induced degradation of the internal interfaces of materials consisting of HA and biodegradable polymers can severely compromise the in vivo mechanical stability of these biocomposites.

Acknowledgement

This work was supported by the National Institutes of Health under Grant No. 5R01 DE015633.

References

[1] Ratner BD. Biomaterials science: an introduction to materials in medicine. San Diego, CA: Academic Press; 1996.
[2] Black J. Biological performance of materials: fundamentals of biocompatibility. Boca Raton, FL: Taylor & Francis; 2006.
[3] Huiskes R, Weinans H, Vanrietbergen B. The relationship between stress shielding and bone-resorption around total hip stems and the effects of flexible materials. Clin Orthop Relat Res 1992:124–34.
[4] Russias J, Saiz E, Deville S, Gryn K, Liu G, Nalla RK, et al. Fabrication and in vitro characterization of three-dimensional organic/inorganic scaffolds by robocasting. J Biomed Mater Res A 2007;83A:434–45.
[5] Russias J, Saiz E, Nalla RK, Tomsia AP. Microspheres as building blocks for HA/polylactide biodegradable composites. J Mater Sci 2006;41:5127–33.
[6] Russias J, Saiz E, Nalla RK, Gryn K, Ritchie RO, Tomsia AP. Fabrication and mechanical properties of PLA/HA composites: a study of in vitro degradation. Mater Sci Eng C 2006;26:1289–95.
[7] Shikinami Y, Okuno M. Bioresorbable devices made of forged composites of HA (HA) particles and poly-L-lactide (PLLA). Part I. Basic characteristics. Biomaterials 1999;20:859–77.
[8] Shikinami Y, Okuno M. Bioresorbable devices made of forged composites of HA (HA) particles and poly-L-lactide (PLLA). Part II. Practical properties of miniscrews and miniplates. Biomaterials 2001;22:3197–211.
[9] Suchanek W, Yoshimura M. Processing and properties of HA-based biomaterials for use as hard tissue replacement implants. J Mater Res 1998;13:94–117.
[10] Rezwan K, Chen QZ, Blaker JJ, Boccaccini AR. Biodegradable and bioactive porous polymer/inorganic composite scaffolds for bone tissue engineering. Biomaterials 2006;27:3413–31.
[11] Lam CXF, Teoh SH, Hutmacher DW. Comparison of the degradation of polycaprolactone and polycaprolactone-(beta-tricalcium phosphate) scaffolds in alkaline medium. Polym Int 2007;56:718–28.
[12] Berkland C, King M, Cox A, Kim K, Pack DW. Precise control of PLG microsphere size provides enhanced control of drug release rate. J Control Release 2002;82:137–47.
[13] Oh JE, Nam YS, Lee KH, Park TG. Conjugation of drug to poly(D,L-lactic-co-glycolic acid) for controlled release from biodegradable microspheres. J Control Release 1999;57:269–80.
[14] Adamson AW, Gast AP. Physical Chemistry of Surfaces. New York: Wiley; 1997.
[15] Becher PF, Sun EY, Hsueh CH, Alexander KB, Hwang SL, Waters SB, et al. Debonding of interfaces between beta-silicon nitride whiskers and Si–Al–Y oxynitride glasses. Acta Mater 1996;44:3881–93.
[16] Wu S. Polymer Interface and Adhesion. New York: Marcel Dekker; 1982.
[17] Blaker JJ, Maquet V, Boccaccini AR, Jerome R, Bismarck A. Wetting of bioactive glass surfaces by poly(alpha-hydroxyacid) melts: interaction between bioglass (R) and biodegradable polymers. E-Polymers 2005;023.
[18] Israelachvili JN. Intermolecular and surface forces. London: Academic Press; 1991.
[19] He MY, Hutchinson JW. Crack deflection at an interface between dissimilar elastic-materials. Intl J Solids Struct 1989;25:1053–67.

[20] Imbeni V, Kruzic JJ, Marshall GW, Marshall SJ, Ritchie RO. The dentin–enamel junction and the fracture of human teeth. Nat Mater 2005;4:229–32.
[21] Klomp JT. Ceramic–metal interactions. Mater Res Soc Sympos Proc 1985;40:381.
[22] Nicholas M, Poole DM, Crispin RM. Strength of metal–alumina interfaces. Am Ceram Soc Bull 1968;47:374.
[23] Hutchinson JW, Suo Z. Mixed-mode cracking in layered materials. Adv Appl Mech 1992;29:63–191.
[24] Cao HC, Thouless MD, Evans AG. Residual-stresses and cracking in brittle solids bonded with a thin ductile layer. Acta Metall Mater 1988;36:2037–46.
[25] Dalgleish BJ, Lu MC, Evans AG. The strength of ceramics bonded with metals. Acta Metall Mater 1988;36:2029–35.
[26] Ritchie RO, Cannon RM, Dalgleish BJ, Dauskardt RH, McNaney JM. Mechanics and mechanisms of crack-growth at or near ceramic–metal interfaces: interface engineering strategies for promoting toughness. Mater Sci Eng A 1993;166:221–35.
[27] Dalgleish BJ, Saiz E, Tomsia AP, Cannon RM, Ritchie RO. Interface formation and strength in ceramic–metal systems. Scripta Metall Mater 1994;31:1109–14.
[28] Thomson RC, Yaszemski MJ, Powers JM, Mikos AG. Fabrication of biodegradable polymer scaffolds to engineer trabecular bone. J Biomat Sci-Polym E 1995;7:23–38.
[29] Karjalainen T, HiljanenVainio M, Malin M, Seppala J. Biodegradable lactone copolymers. 3. Mechanical properties of e-caprolactone and lactide copolymers after hydrolysis in vitro. J Appl Polym Sci 1996;59:1299–304.
[30] Migliaresi C, Fambri L, Cohn D. A study on the in-vitro degradation of poly(lactic acid). J Biomat Sci-Polym E 1994;5:591–606.
[31] Marra KG, Szem JW, Kumta PN, DiMilla PA, Weiss LE. In vitro analysis of biodegradable polymer blend/HA composites for bone tissue engineering. J Biomed Mater Res 1999;47:324–35.
[32] Chrissafis K, Antoniadis G, Paraskevopoulos KM, Vassiliou A, Bikiaris DN. Comparative study of the effect of different nanoparticles on the mechanical properties and thermal degradation mechanism of in situ prepared poly(e-caprolactone) nanocomposites. Compos Sci Technol 2007;67:2165–74.
[33] Jones DS, Djokic J, McCoy CP, Gorman SP. poly(ε-caprolactone) and poly(ε-caprolactone)–polyvinylpyrrolidone–iodine blends as ureteral biomaterials: characterisation of mechanical and surface properties, degradation and resistance to encrustation in vitro. Biomaterials 2002;23:4449–58.
[34] Goldberg D. A review of the biodegradability and utility of poly(caprolactone). J Environ Polym Degrad 1995;3:61–7.
[35] Suchanek W, Yashima M, Kakihana M, Yoshimura M. Hydroxyapatite ceramics with selected sintering additives. Biomaterials 1997;18:923–33.